

International Conference on Recent Trends in Applied Mathematical Sciences (ICRTAMS-2020)

Tiruvannamalai, India • 26–27 September 2020

Editors • M. Seenivasan, K. Pattabiraman and A. Vadivel

AIP
Publishing

September 2021

INTERNATIONAL CONFERENCE ON RECENT TRENDS IN APPLIED MATHEMATICAL SCIENCES (ICRTAMS-2020)

[Close](#)



• Table of Contents

INTERNATIONAL CONFERENCE ON RECENT TRENDS IN APPLIED MATHEMATICAL SCIENCES (ICRTAMS-2020)

< PREV NEXT >



Conference date: 26–27 September 2020

Location: Tiruvannamalai, India

ISBN: 978-0-7354-4122-4

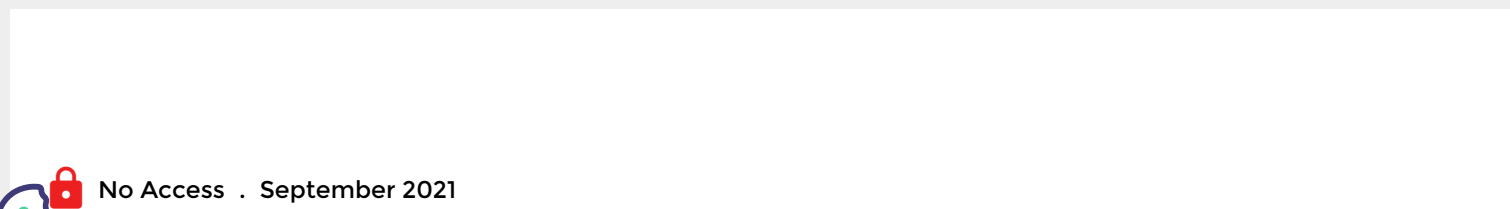
Editors: M. Seenivasan, K. Pattabiraman and A. Vadivel

Volume number: 2364

Published: Sep 23, 2021

DISPLAY : 20 50 100 all

PRELIMINARY




Preface: International Conference on Recent Trends in Applied Mathematical Sciences (ICRTAMS-2020)

AIP Conference Proceedings **2364**, 010001 (2021); <https://doi.org/10.1063/12.0005684>



MATHEMATICS

 No Access . September 2021


Fixed point theorems of generalized $(\kappa, \mu)_s$ - rational contractive mappings in ordered complex valued quasi b - metric spaces with application

J. Uma Maheswari, M. Ravichandran and A. Anbarasan

AIP Conference Proceedings **2364**, 020001 (2021); <https://doi.org/10.1063/5.0064248>

SHOW ABSTRACT



 No Access . September 2021


Prime labeling for some bistar related graphs

T. Malathi and K. Balasangu

AIP Conference Proceedings **2364**, 020002 (2021); <https://doi.org/10.1063/5.0064375>

SHOW ABSTRACT




 No Access . September 2021



SHOW ABSTRACT




 No Access . September 2021

An analytic expression for the frontal flow period in 1D counter-current imbibition including dynamic capillary pressure into saturated homogeneous porous media

Saroj R. Yadav and Vishnu Narayan Mishra

SHOW ABSTRACT




 No Access . September 2021

Solution for *ABC*-fractional order neutral impulsive differential equation with finite delay

Ramalingam Devipriya and Sellappan Selvi

SHOW ABSTRACT



 No Access . September 2021


Triple connected eternal domination number of different product of paths and cycles

T. Ponnuchamy, G. Mahadevan and Selvam Avadayappan



SHOW ABSTRACT



 No Access . September 2021


Equality on restrained step domination number of a graph

M. Vimala Suganthi and G. Mahadevan

AIP Conference Proceedings **2364**, 020007 (2021); <https://doi.org/10.1063/5.0063487>

SHOW ABSTRACT



 No Access . September 2021


ATES domination in number for some graph operations

S. Anuthiya and G. Mahadevan

AIP Conference Proceedings **2364**, 020008 (2021); <https://doi.org/10.1063/5.0063406>

SHOW ABSTRACT



 No Access . September 2021


Implication operation on picture fuzzy matrices

P. Murugadas

AIP Conference Proceedings **2364**, 020009 (2021); <https://doi.org/10.1063/5.0063580>

SHOW ABSTRACT



 No Access . September 2021


Minimal and maximal Z -open sets in nano topological spaces

X. Arul Selvaraj and U. Balakrishna

AIP Conference Proceedings **2364**, 020010 (2021); <https://doi.org/10.1063/5.0062906>

SHOW ABSTRACT



 No Access . September 2021


Some (δ, γ) -fuzzy homomorphism theorem on rings

J. Jayaraj, X. Arul Selvaraj and S. Rexlin Jeyakumari

AIP Conference Proceedings **2364**, 020011 (2021); <https://doi.org/10.1063/5.0062910>

SHOW ABSTRACT



 No Access . September 2021


Optimization of EOQ model without shortages under uncertainty

X. Arul Selvaraj, J. Jayaraj, I. Shiny Bridgett and S. Rexlin Jeyakumari

AIP Conference Proceedings **2364**, 020012 (2021); <https://doi.org/10.1063/5.0062915>

SHOW ABSTRACT



 No Access . September 2021

Optimization of fuzzy inventory model using Kuhn – Tucker technique and Lagrangean method


J. Jayaraj, X. Arul Selvaraj, I. Shiny Bridgett and S. Rexlin Jeyakumari

AIP Conference Proceedings **2364**, 020013 (2021); <https://doi.org/10.1063/5.0062917>

 BROWSE VOLUMES

SHOW ABSTRACT



 No Access . September 2021


Triangular norm (δ, γ) - fuzzy interior-ideals of hemi rings and its properties

X. Arul Selvaraj, J. Jayaraj and S. Rexlin Jeyakumari

AIP Conference Proceedings **2364**, 020014 (2021); <https://doi.org/10.1063/5.0062917>

SHOW ABSTRACT



 No Access . September 2021


Neutrosophic positive implicative AAA-ideals in KU -algebras

M. Vasu and D. Ramesh Kumar

AIP Conference Proceedings **2364**, 020015 (2021); <https://doi.org/10.1063/5.0062904>

SHOW ABSTRACT



 No Access . September 2021


Neutrosophic e -open maps, neutrosophic e -closed maps and neutrosophic e -homeomorphisms in neutrosophic topological spaces

A. Vadivel, P. Thangaraja and C. John Sundar

AIP Conference Proceedings **2364**, 020016 (2021); <https://doi.org/10.1063/5.0062880>

SHOW ABSTRACT



 No Access . September 2021


Some topological operations and $N_{nc} Z^*$ continuity in N_{nc} topological spaces

K. Balasubramaniyan, A. Gobikrishnan and A. Vadivel

AIP Conference Proceedings **2364**, 020017 (2021); <https://doi.org/10.1063/5.0063130>

SHOW ABSTRACT



 No Access . September 2021


On $N_{nc} Z^*$ -open and $N_{nc} Z^*$ -closed functions

K. Balasubramaniyan, A. Gobikrishnan and A. Vadivel

AIP Conference Proceedings **2364**, 020018 (2021); <https://doi.org/10.1063/5.0063132>

SHOW ABSTRACT



 No Access . September 2021


Characterizations of $N_{nc} Z^*$ -open and $N_{nc} Z^*$ -closed functions

K. Balasubramaniyan and A. Gobikrishnan

AIP Conference Proceedings **2364**, 020019 (2021); <https://doi.org/10.1063/5.0063133>

SHOW ABSTRACT



 No Access . September 2021

Neutrosophic Z -continuous maps and Z -irresolute maps


N. Moogambigai, A. Vadivel and S. Tamilselvan

AIP Conference Proceedings **2364**, 020020 (2021); <https://doi.org/10.1063/5.0063135>

 BROWSE VOLUMES

SHOW ABSTRACT



 No Access . September 2021


Convergence of the power sequence of a monotone increasing neutrosophic soft matrix

M. Kavitha and P. Murugadas

AIP Conference Proceedings **2364**, 020021 (2021); <https://doi.org/10.1063/5.0063408>

SHOW ABSTRACT



 No Access . September 2021


Strongly faint N_{nc} e-continuous function in N_{nc} topological spaces

V. Sudha, A. Vadivel and S. Tamilselvan

AIP Conference Proceedings **2364**, 020022 (2021); <https://doi.org/10.1063/5.0062886>

SHOW ABSTRACT



 No Access . September 2021


Characterizations of quasi N_{nc} e-open (closed) functions in N_{nc} topological spaces

V. Sudha and S. Tamilselvan

AIP Conference Proceedings **2364**, 020023 (2021); <https://doi.org/10.1063/5.0062887>

SHOW ABSTRACT



 No Access . September 2021


Higher-order fractional programming problem and their duality theorems in vector optimization with cone- η – invex functions

Tarun Kumar Gupta, Rajesh Kumar Tripathi, Chetan Swarup, Kuldeep Singh, Ramu Dubey and Vishnu Narayan Mishra

AIP Conference Proceedings **2364**, 020024 (2021); <https://doi.org/10.1063/5.0063229>

SHOW ABSTRACT



 No Access . September 2021


Fuzzy reliability evaluation of complex systems with Monte Carlo simulation

M. K. Sharma, Harendra Yadav, Nitesh Dhiman and Vishnunarayan Mishra

AIP Conference Proceedings **2364**, 020025 (2021); <https://doi.org/10.1063/5.0062861>

SHOW ABSTRACT



 No Access . September 2021

Digital color-image encryption scheme based on elliptic curve cryptography ElGamal encryption and 3D Lorenz map

Dhanesh Kumar, Anand B. Joshi, Sonali Singh and Vishnu Narayan Mishra

AIP Conference Proceedings **2364**, 020026 (2021); <https://doi.org/10.1063/5.0062877>

SHOW ABSTRACT




Getting a job is a tough job: A mathematical model

Harendra Verma, Neha Mathur, Vishnu Narayan Mishra and Pankaj Mathur

AIP Conference Proceedings **2364**, 020027 (2021); <https://doi.org/10.1063/5.0062996>

SHOW ABSTRACT



 No Access . September 2021


Inverse theorems for some linear positive operators using Beta and Baskakov basis functions

Lakshmi Narayan Mishra, A. Srivastava, T. Khan, S. A. Khan and Vishnu Narayan Mishra

AIP Conference Proceedings **2364**, 020028 (2021); <https://doi.org/10.1063/5.0062925>

SHOW ABSTRACT



 No Access . September 2021


Mediative neuro fuzzy inference and mediative fuzzy expert system for the identification of severity diagnosis of the dengue patients

M. K. Sharma, Nitesh Dhiman, Snehlata Verma and Vishnu Narayan Mishra

AIP Conference Proceedings **2364**, 020029 (2021); <https://doi.org/10.1063/5.0062862>

SHOW ABSTRACT



 No Access . September 2021

Non linear \mathcal{L} - fuzzy stability of functional equations in various spaces

Jyotsana, Renu Chugh, Ramu Dubey and Vishnu Narayan Mishra


AIP Conference Proceedings **2364**, 020030 (2021); <https://doi.org/10.1063/5.0062959>

BROWSE VOLUMES



SHOW ABSTRACT



 No Access . September 2021


Non-differentiable higher-order fractional programming problem and their duality results under cone-invex functions

Rajesh Kumar Tripathi, Arvind Kumar, Ramu Dubey, Awanish Kumar Tiwari, Jasvendra Tyagi and Vishnu Narayan Mishra

AIP Conference Proceedings **2364**, 020031 (2021); <https://doi.org/10.1063/5.0063227>

SHOW ABSTRACT



 No Access . September 2021


Symmetric spaces approach to some fixed function results

Savita Rathee, Priyanka Gupta and Lakshmi Narayan Mishra

AIP Conference Proceedings **2364**, 020032 (2021); <https://doi.org/10.1063/5.0063590>

SHOW ABSTRACT



 No Access . September 2021


Wardowski type cyclic F -contraction mappings in orthogonal metric spaces and some proximity point results

Raju Roy, Nilakshi Goswami, Lakshmi Narayan Mishra and Vishnu Narayan Mishra

AIP Conference Proceedings **2364**, 020033 (2021); <https://doi.org/10.1063/5.0062892>

SHOW ABSTRACT



 No Access . September 2021


Analysis of queueing model with catastrophe and restoration

M. Seenivasan, M. Kameswari, V. J. Chakravarthy and M. Indumathi

AIP Conference Proceedings **2364**, 020034 (2021); <https://doi.org/10.1063/5.0062890>

SHOW ABSTRACT



 No Access . September 2021


Parabolic fuzzy variables and their some properties: A comparative SWOT up

Palash Dutta and Tabendra Nath Das

AIP Conference Proceedings **2364**, 020035 (2021); <https://doi.org/10.1063/5.0062840>

SHOW ABSTRACT



 No Access . September 2021

Performance analysis of multi-server markovian queue with intermittently available and unreliable server

M. Seenivasan and K. S. Subasri

AIP Conference Proceedings **2364**, 020036 (2021); <https://doi.org/10.1063/5.0062891>

SHOW ABSTRACT



Z-open sets in nano topological spaces


X. Arul Selvaraj and U. Balakrishna

AIP Conference Proceedings **2364**, 020037 (2021); <https://doi.org/10.1063/5.0062907>

SHOW ABSTRACT



MECHANICAL ENGINEERING

 No Access . September 2021


Efficiency and effectiveness of a fin having the ellipse cross section in the unsteady state condition

Petrus Kanisius Purwadi, Budi Setyahandana and Michael Seen

AIP Conference Proceedings **2364**, 030001 (2021); <https://doi.org/10.1063/5.0063541>

SHOW ABSTRACT



 No Access . September 2021


TRNSYS simulation analysis of basin-type solar still

Mikhael G. Haribawono, Wisnu J. Wicaksono and F. A. Rusdi Sambada

AIP Conference Proceedings **2364**, 030002 (2021); <https://doi.org/10.1063/5.0062855>

SHOW ABSTRACT



 No Access . September 2021



Effect of wick color on solar still performance with cylindrical absorber


Henrikus Oscar Diaz Adenover, Juan Vitalis Alfiano Bramantyo and F. A. Rusdi Sambada

AIP Conference Proceedings **2364**, 030003 (2021); <https://doi.org/10.1063/5.0062854>

SHOW ABSTRACT



CHEMISTRY

 No Access . September 2021


Synthesis and DFT calculation of novel pyrazole derivatives

S. Priyanka, S. Sivapriya, D. Sivakumar, M. Gopalakrishnan, M. Seenivasan and H. Manikandan

AIP Conference Proceedings **2364**, 040001 (2021); <https://doi.org/10.1063/5.0063016>

SHOW ABSTRACT



 No Access . September 2021

Experimental and optimized studies of some pyrimidine derivatives

S. Sivapriya, S. Priyanka, D. Sivakumar, M. Gopalakrishnan, M. Seenivasan and H. Manikandan

AIP Conference Proceedings **2364**, 040002 (2021); <https://doi.org/10.1063/5.0063017>

SHOW ABSTRACT



TRNSYS simulation analysis of basin-type solar still

Cite as: AIP Conference Proceedings **2364**, 030002 (2021); <https://doi.org/10.1063/5.0062855>
Published Online: 23 September 2021

Mikhael G. Haribawono, Wisnu J. Wicaksono, and F. A. Rusdi Sambada



View Online



Export Citation

ARTICLES YOU MAY BE INTERESTED IN

[Effect of wick color on solar still performance with cylindrical absorber](#)

AIP Conference Proceedings **2364**, 030003 (2021); <https://doi.org/10.1063/5.0062854>

[The effect of Ni doping in powder-in-tube-MgB₂ material](#)

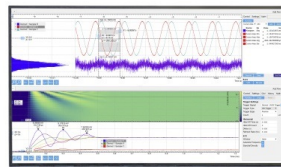
AIP Conference Proceedings **2382**, 020002 (2021); <https://doi.org/10.1063/5.0059999>

[Simulation study of size and aggregation effect on colorimetric spherical gold nanoparticles](#)

AIP Conference Proceedings **2382**, 080001 (2021); <https://doi.org/10.1063/5.0059983>

Challenge us.

What are your needs for
periodic signal detection?



Zurich
Instruments



TRNSYS Simulation Analysis of Basin-Type Solar Still

Mikhael G. Haribawono^{1, a)}, Wisnu J. Wicaksono^{1, b)} and F. A. Rusdi Sambada¹

¹*Department of Mechanical Engineering, Sanata Dharma University,
Yogyakarta, Indonesia*

^{a)}Corresponding Author: mikhaelgibran@gmail.com

^{b)}wisnujep@gmail.com

Abstract. Conventional basin-type solar still (CSS) is the simplest type of solar water distillation system. In this study, CSS was modeled and simulated. The effect of variations in water mass inside the basin, absorber absorptivity, glass absorptivity, glass reflectivity and heat loss coefficient were investigated. Finally, the system was simulated using the same data of solar radiation intensity, ambient temperature and wind speed in each variation and the highest distilled water results are 2.33 kg in water mass inside the basin variation of 5 kg, absorber absorptivity variation of 0.9, glass absorptivity variation of 0.06, glass reflectivity variation of 0.08 and heat loss coefficient variation of 14 W/(m².K). Overall study shows that TRNSYS is a very useful tool for design and parameter analysis of solar water distillation system.

Key words: Simulation, Distillation, Solar Still.

INTRODUCTION

The demand for clean water continues to increase due to the increasing population and rapid industrial growth worldwide, while the availability of drinking water is also decreasing day by day. Clean water is needed for household, industrial and agricultural purposes [1]. Drinking water is indispensable for life and its scarcity continues to increase worldwide, especially in arid regions and modern industrial areas. Similar problems occur in remote areas and islands where freshwater supply is obtained through expensive transportation [2]. On the other hand, seawater is abundant in many parts of the world but requires the removal of salinity at the added cost of energy, which is another scarce resource. One of the solutions to solve this problem is to provide several sources of sustainable water distillation. Therefore, solar energy will be a potential choice to become a source of energy for water distillation in these places [3].

The working principle of solar distillation is based on a natural phenomenon. The water in oceans, rivers and lakes evaporates as it is heated by solar energy. Water vapor reaches the atmosphere and condenses, then falls back down as rainwater. The conventional basin-type solar still (CSS) recreate this natural phenomenon on a small scale. CSS system is the most common method for solar water distillation [4]. The CSS is basically an insulated basin filled with shallow uniform temperature contaminated water heated by absorption of incoming solar radiation through the transparent condensing glass pane on the top [5].

Another problem that exists is the low efficiency of this solar water distillation system. Thus, many studies have been conducted to improve the performance of CSS. Some researchers suggest the addition of a sensible heat energy storage in the form of knitted jute cloth wrapped over the entire surface of the heat-storing sand material to increase the CSS performance. It was found that the water temperature in the CSS with sensible heat energy storage was 25% higher than the CSS without sensible heat energy storage and the yield of clean water in the CSS with and without sensible heat energy storage was 5,9 kg/m² and 5,5 kg/m² respectively [6]. Other variations have also been researched, such as in the double slope basin-type with multi-wick solar still. The result indicates that the thermal efficiencies of the solar still with the addition of jute and black cotton wicks are 20.94% and 23.03% [7]. Another study has been carried out to show the CSS performance compared with the CSS modified with 100 sand-filled cotton bags (MSS).

The overall efficiency of MSS for 30 kg and 40 kg basin water is improved by 28.96% and 31.31% compared with the CSS [8]. Apart from experimental research, there is also analytical research using simulations from various software. Some researchers have analyzed the CSS using ANSYS CFX with the processes of condensation and evaporation in the solar still made in a two-phase three-dimensional model. The obtained simulation results of distillate output are compatible with experimental results [9]. Other researchers have modeled and simulated an Inclined Solar Water Distillation (ISWD) system with the effects of feed water mass flow rate and solar radiation intensity on the system parameters were investigated. The simulation results are compatible with the experimental results [10]. The advantage of simulation is that there is no need to physically change the solar still device to achieve the cost savings. The simulation results can show the characteristics of each type of solar still, which can be used as a reference in designing the most efficient solar still system. In this study, a simulation will be carried out using TRNSYS by making a mathematical model of the CSS.

MATHEMATICAL MODEL

This section will discuss the mathematical modeling used in simulation analysis. Here we use the units as follow: energy and heat loss are measured in W/m^2 , temperature in $^{\circ}C$, distilled water mass evaporation rate in $kg/(second.m^2)$, convection heat transfer coefficient and total heat transfer coefficient in $W/(m^2.^{\circ}C)$, the partial pressure of vapor in Pa, wind speed in m/s, mass in kg, heat capacity in $J/(kg.^{\circ}C)$, temperature changes in $^{\circ}C$ and time changes in second.

The efficiency of the solar still is the ratio between solar energy that can be used for the evaporation process with solar energy received by the solar still, formulated as

$$\eta = \frac{q_e}{I(t)}, \quad (1)$$

where q_e is the portion of solar energy that can be used for the evaporation process and $I(t)$ is the solar energy received by the solar still. The distilled water mass evaporation rate is obtained from

$$dm_c = \frac{q_e}{h_{fg}}, \quad (2)$$

where dm_c is the distilled water mass evaporation rate and h_{fg} is the latent heat of water evaporation.

There are many types of solar still and the conventional (basin) is the simplest type (Figure 1).

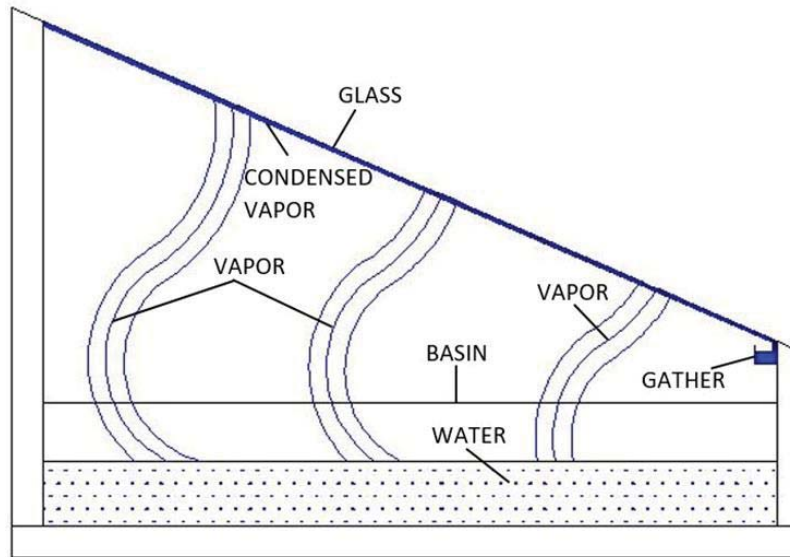


FIGURE 1. The distillation process of the CSS

Solar energy absorbed by the basin will transfer to the water inside the basin by convection. The energy that transfers by convection from the basin to the water is obtained from

$$q = h(T_1 - T_2), \quad (3)$$

where q is the amount of energy that is convected from the basin to the water (q_{cb}), h is the convection heat transfer coefficient from the basin to the water (h_{cb}), T_1 is the basin temperature (T_b) and T_2 is the water temperature inside the basin (T_w). Some energy received by water inside the basin is used for the water evaporation and some will transfer to the glass by convection and radiation. The amount of energy radiated to the glass is obtained from

$$q_r = \frac{\sigma[(T_1 + 273,15)^4 - (T_2 + 273,15)^4]}{\frac{1}{\varepsilon_1} + \frac{1}{\varepsilon_2} - 1}, \quad (4)$$

where σ is the Stefan-Boltzmann constant ($5,67 \times 10^{-8} \text{ W}/(\text{m}^2 \cdot \text{K}^4)$), T_1 is the water temperature (T_w), T_2 is the glass temperature (T_g), ε_1 is the water emissivity (ε_w) and ε_2 is the glass emissivity (ε_g). The amount of energy convected to the glass is obtained from equation (3) where q is the amount of energy convected to the glass (q_c), h is the convection heat transfer coefficient from the water to the glass (h_c), T_1 is the water temperature (T_w) and T_2 is the glass temperature (T_g). Convection heat transfer coefficient (h_c) formulated as

$$h_c = 0,884 \left[T_w - T_g + \frac{(P_w - P_g)(T_w + 273,15)}{268,9 \times 10^3 - P_w} \right]^{1/3}, \quad (5)$$

where T_w is the water temperature, T_g is the glass temperature, P_w is the partial pressure of vapor at water temperature and P_g is the partial pressure of vapor at glass temperature. The energy used for water evaporation formulated as

$$q_e = 16,273 \times 10^{-3} \cdot h_c \cdot (P_w - P_g). \quad (6)$$

The heat energy received by the glass from the water is the energy of water evaporation, the energy that is convected and radiated from the water to the glass will be discharged to the surrounding environment by convection and radiation. The amount of heat energy discharged by glass into the environment by convection is calculated using equation (3) where q is the amount of energy discharged by convection into the environment (q_{cg}), h is the convection heat transfer coefficient from the glass into the environment (h_{cg}), T_1 is the glass temperature (T_g) and T_2 is the ambient temperature (T_a). Convection heat transfer coefficient from the glass into the environment (h_{cg}) is obtained from

$$h_{cg} = 5,7 + 3,8V_a, \quad (7)$$

where V_a is wind speed. The amount of heat energy discharged into the environment by radiation is obtained from the equation (4) where T_1 is the glass temperature (T_g), T_2 is the sky temperature (T_{sky}), ε_1 is the glass emissivity (ε_g) and ε_2 is the sky emissivity ($\varepsilon_{sky} \approx 1$). The sky temperature (T_{sky}) is obtained from

$$T_{sky} = T_a - 6, \quad (8)$$

where T_a is the ambient temperature.

The heat energy loss dramatically affects the efficiency of solar still. It occurs because of the temperature difference between the solar still and the ambient temperature. Insulation material and geometry, the quality of the material and the solar still device, and wind speed greatly influence the magnitude of the heat energy loss. The amount of heat loss is calculated by the equation (3) where q is the amount of heat loss (q_l), h is the total heat transfer coefficient from the basin into the environment (U_b), T_1 is the basin temperature (T_b) and T_2 is the ambient temperature (T_a).

Energy Balance in the CSS

The energy balance equation can express the process that occurs in a solar still device. The energy balance equation in the solar still produces a system of first-order differential equations, which is a function of the temperature of all parts of the solar still device (glass, cooling water, distilled water and absorber). The system of equations is solved to get the temperature in each part of the solar still device in each time range of data collection. The temperatures obtained are used to determine the performance of the solar still device (yield of distilled water and efficiency) and other influencing parameters.

The energy balance in the CSS is divided based on the parts of the device (Figure 2), which are basin, water inside the basin and glass.

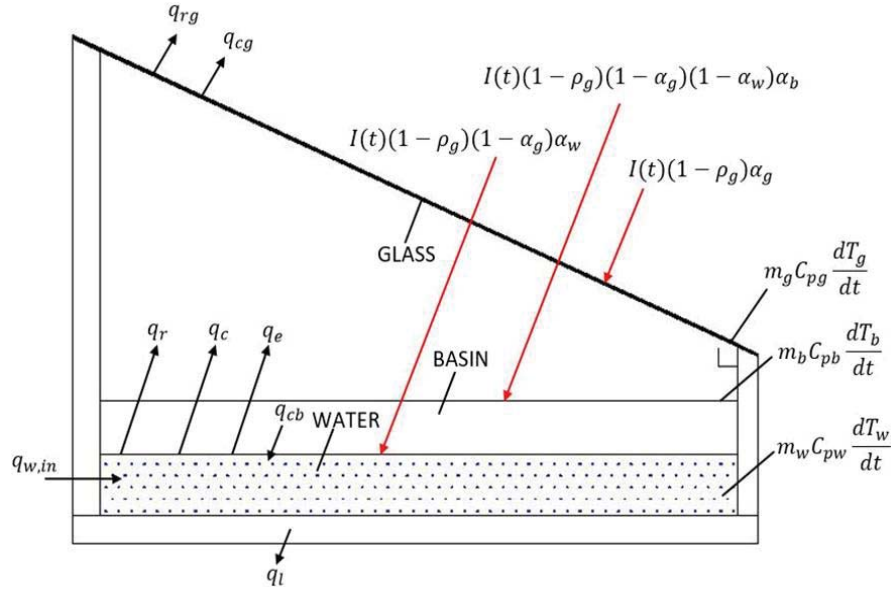


FIGURE 2. The energy balance in the CSS

Energy Balance in the Glass

The energy stored in the glass = the energy that goes into the glass – the energy that goes out of the glass,

$$m_g C_{pg} \frac{dT_g}{dt} = I(t)(1 - \rho_g)\alpha_g + q_r + q_c + q_e - q_{cg} - q_{rg}, \quad (9)$$

where m_g is the glass mass, C_{pg} is the glass heat capacity, dT_g is the change in temperature of the glass, dt is the change in time, $I(t)$ is the incoming solar energy, ρ_g is the glass reflectivity, α_g is the glass absorptivity, q_r is the energy radiated from the water to the glass, q_c is the energy that is convected from the water to the glass, q_e is the energy used for water evaporation, q_{cg} is the energy that is convected from the glass into the environment and q_{rg} is the energy radiated from the glass into the environment. $I(t)$, q_r , q_c and q_e is the energy that goes into the glass, while q_{cg} and q_{rg} is the energy that goes out of the glass.

Energy Balance in the Water Inside the Basin

The energy stored in the water = the energy that goes into the water – the energy that goes out of the water,

$$m_w C_{pw} \frac{dT_w}{dt} = I(t)(1 - \rho_g)(1 - \alpha_g)\alpha_w + q_{cb} - q_r - q_c - q_e + q_{w,in}, \quad (10)$$

where m_w is the water mass, C_{pw} is the water heat capacity, dT_w is the change in temperature of the water, dt is the change in time, $I(t)$ is the incoming solar energy, ρ_g is the glass reflectivity, α_g is the glass absorptivity, α_w is the water absorptivity, q_{cb} is the energy that is convected from the basin to the water, q_r is the energy radiated from the water to the glass, q_c is the energy convected from the water to the glass, q_e is the energy used for water evaporation and $q_{w,in}$ is the energy that transfers from the water inside the basin to the incoming distilled water. $I(t)$ and q_{cb} is the energy that goes into the water, while q_r , q_c , q_e and $q_{w,in}$ is the energy that goes out of the water.

Energy Balance in the Basin

The energy stored in the basin = the energy that goes into the basin – the energy that goes out of the basin,

$$m_b C_{pb} \frac{dT_b}{dt} = I(t)(1 - \rho_g)(1 - \alpha_g)(1 - \alpha_w)\alpha_b - q_{cb} - q_l, \quad (11)$$

where m_b is the basin mass, C_{pb} is the basin heat capacity, dT_b is the change in temperature of the basin, dt is the change in time, $I(t)$ is the incoming solar energy, ρ_g is the glass reflectivity, α_g is the glass absorptivity, α_w is the water absorptivity, α_b is the basin absorptivity, q_{cb} is the energy that is convected from the basin to the water and q_l is the energy convected from the device into the environment. $I(t)$ is the energy that goes into the basin, while q_{cb} and q_l is the energy that goes out of the basin.

The system of energy balance differential equations in CSS is formulated as

$$T_g = T_g + \frac{dT_g}{dt} dt, \quad (12)$$

$$T_w = T_w + \frac{dT_w}{dt} dt, \quad (13)$$

$$T_b = T_b + \frac{dT_b}{dt} dt. \quad (14)$$

The mathematical solution of the equations system is carried out by substitution and integration factors in the differential equation in each part of the device. Numerical solutions are carried out using the Euler or Runge-Kutta method.

SIMULATION ANALYSIS OF THE CSS

Simulation analysis was performed using TRNSYS, a simulation program mainly used in the renewable energy engineering field and building simulation for solar designs. TRNSYS consists of two parts. The first part is an engine (called the kernel) where the input file is read and processed, the system is solved repeatedly, the convergence is determined and the system variables are plotted. The second part is an extensive library of components, where each of which components models each part of the system's performance. TRNSYS also accommodates utilities that reverse matrices, insert external data files and define thermophysical properties. Users are able to customize existing components or write their own [11].

Simulation Program and Investigated Parameters

The program we used in the simulation was made in the Fortran language. The CSS program is linked to the Type61Basin icon in the TRNSYS software (Figure 3). The program to enter the input data for solar radiation intensity, ambient temperature and wind speed is linked to the TYPE9c icon. The calculation program for the mathematical model used in the simulation is linked to the TYPE16a icon, the program for the sum of the yield distilled water output data is linked to the TYPE55 icon, the program for the graphic creation of the output data results is linked to the TYPE65-2 icon and the program for the table creation of the output data results is linked to the TYPE25c icon.

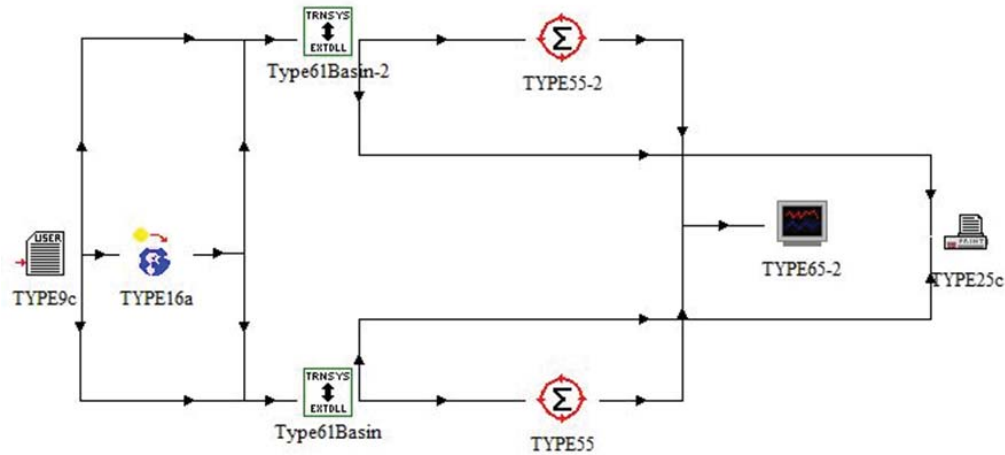


FIGURE 3. TRNSYS scheme used in the simulation

The investigated parameters in this simulation are given in Table 1-5. We carried out five variations in this simulation, which are variations in water mass inside the basin, absorber absorptivity, glass absorptivity, glass reflectivity and heat loss coefficient. The results of this simulation can be used as a reference in designing the most efficient solar still system.

TABLE 1. Investigated parameters of the water mass variation

Parameters	Variation 1	Variation 2	Variation 3
Water mass	5 kg	10 kg	15 kg
Absorber absorptivity	0.9	0.9	0.9
Glass absorptivity	0.06	0.06	0.06
Glass reflectivity	0.08	0.08	0.08
Heat loss coefficient	14 W/(m ² .K)	14 W/(m ² .K)	14 W/(m ² .K)

TABLE 2. Investigated parameters of the absorber absorptivity variation

Parameters	Variation 1	Variation 2	Variation 3
Water mass	5 kg	5 kg	5 kg
Absorber absorptivity	0.9	0.7	0.5
Glass absorptivity	0.06	0.06	0.06
Glass reflectivity	0.08	0.08	0.08
Heat loss coefficient	14 W/(m ² .K)	14 W/(m ² .K)	14 W/(m ² .K)

TABLE 3. Investigated parameters of the glass absorptivity variation

Parameters	Variation 1	Variation 2	Variation 3
Water mass	5 kg	5 kg	5 kg
Absorber absorptivity	0.9	0.9	0.9
Glass absorptivity	0.06	0.08	0.10
Glass reflectivity	0.08	0.08	0.08
Heat loss coefficient	14 W/(m ² .K)	14 W/(m ² .K)	14 W/(m ² .K)

TABLE 4. Investigated parameters of the glass reflectivity variation

Parameters	Variation 1	Variation 2	Variation 3
Water mass	5 kg	5 kg	5 kg
Absorber absorptivity	0.9	0.9	0.9
Glass absorptivity	0.06	0.06	0.06
Glass reflectivity	0.08	0.10	0.15
Heat loss coefficient	14 W/(m ² .K)	14 W/(m ² .K)	14 W/(m ² .K)

TABLE 5. Investigated parameters of the heat loss coefficient variation

Parameters	Variation 1	Variation 2	Variation 3
Water mass	5 kg	5 kg	5 kg
Absorber absorptivity	0.9	0.9	0.9
Glass absorptivity	0.06	0.06	0.06
Glass reflectivity	0.08	0.08	0.08
Heat loss coefficient	14 W/(m ² .K)	20 W/(m ² .K)	25 W/(m ² .K)

Simulation Analysis

The solar radiation intensity, wind speed and ambient temperature used in this simulation are the same in each variation (Figure 4-6).

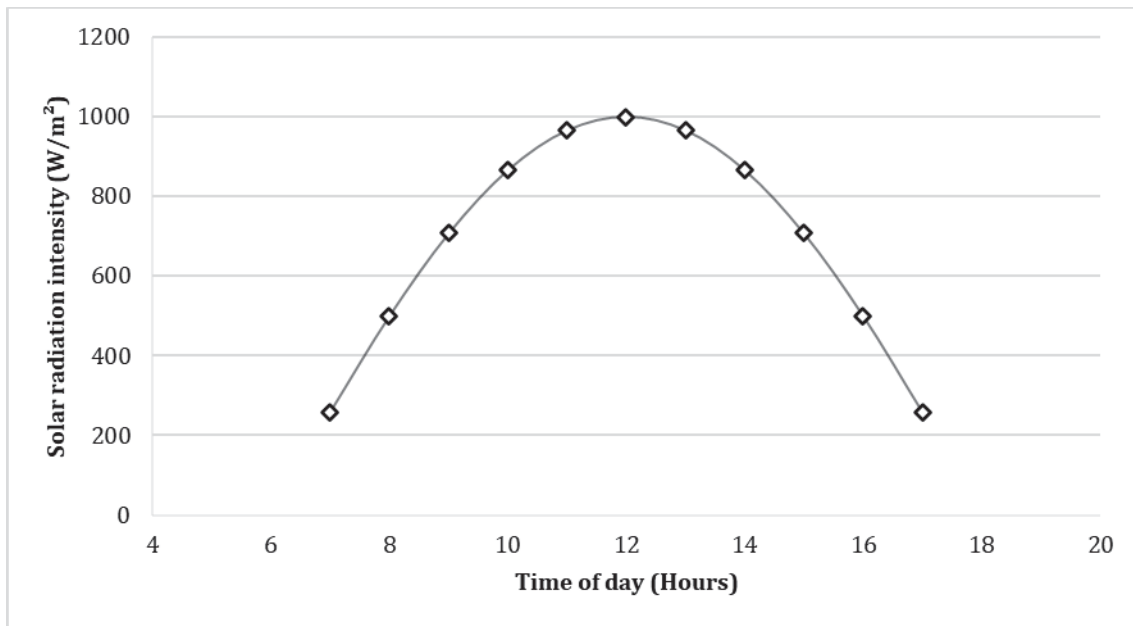


FIGURE 4. Solar radiation intensity used in this simulation

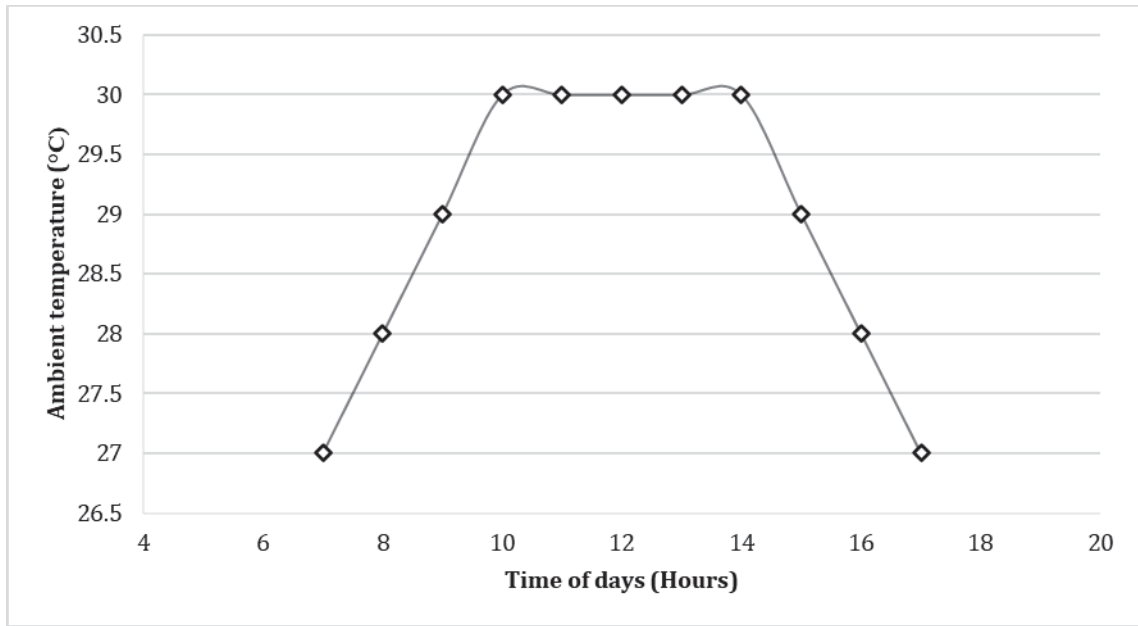


FIGURE 5. Ambient temperature used in this simulation

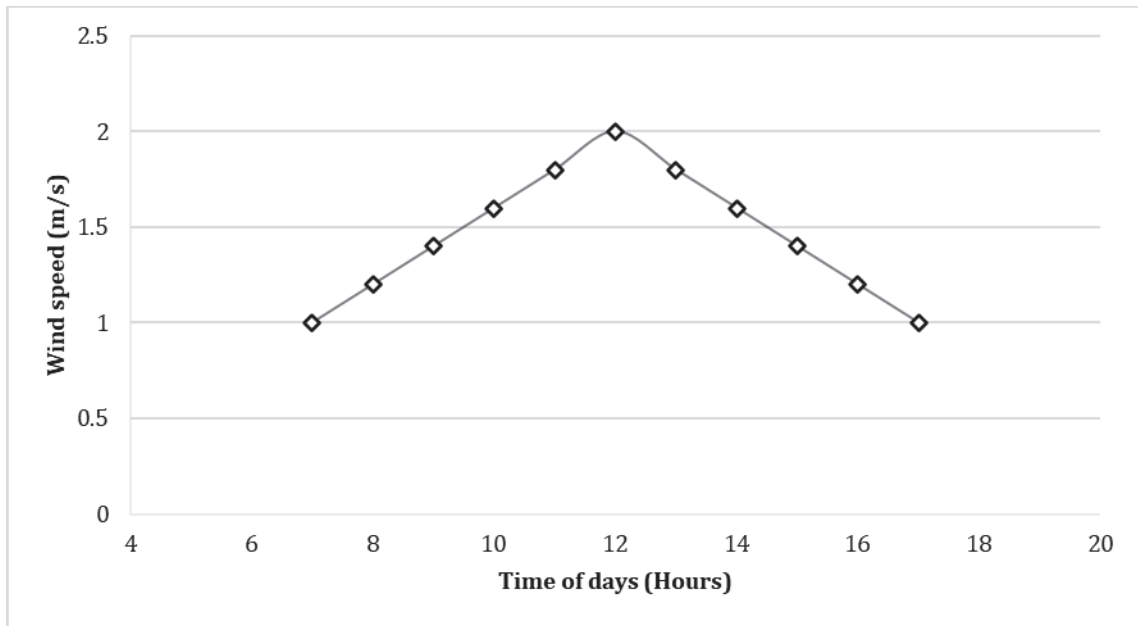


FIGURE 6. Wind speed used in this simulation

The obtained simulation results (Figure 7-11):

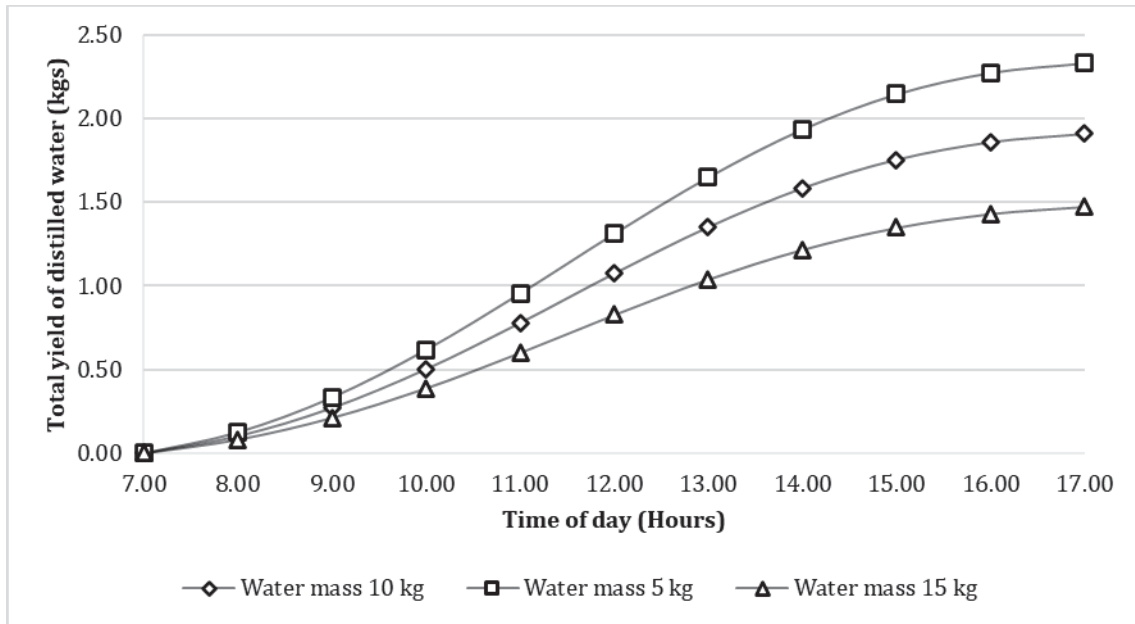


FIGURE 7. The total yield of distilled water from the water mass variation

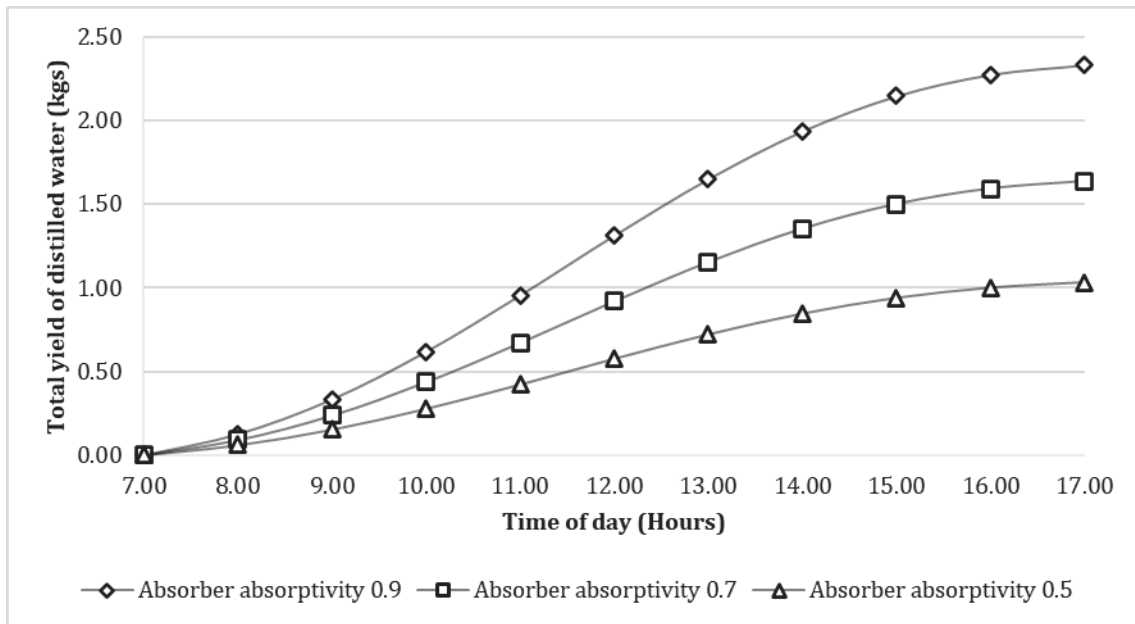


FIGURE 8. The total yield of distilled water from the absorber absorptivity variation

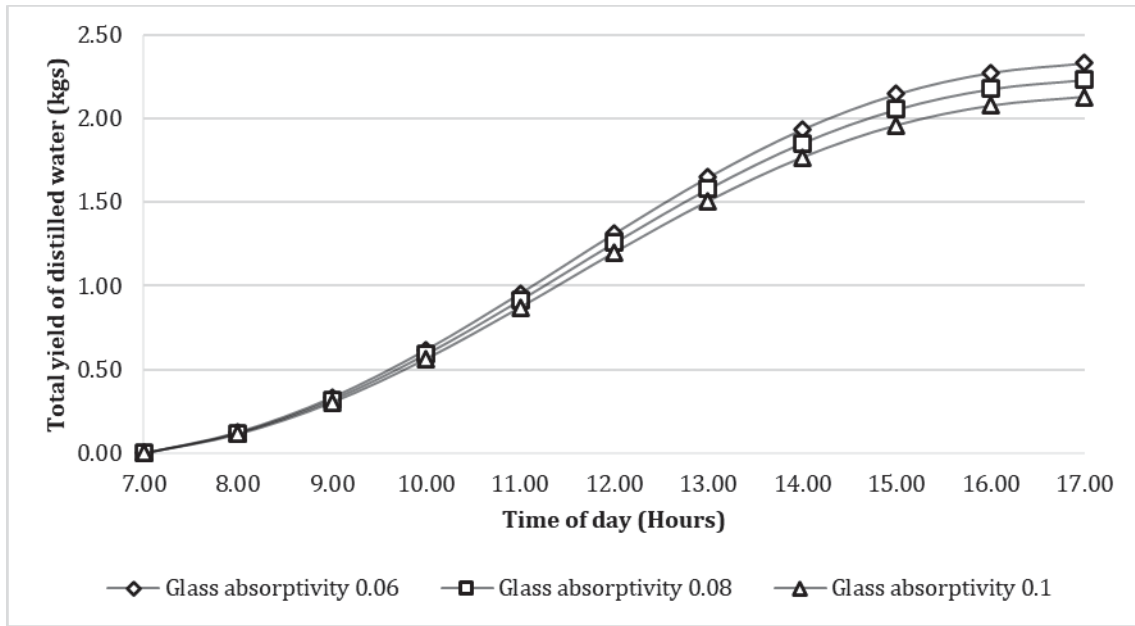


FIGURE 9. The total yield of distilled water from the glass absorptivity variation

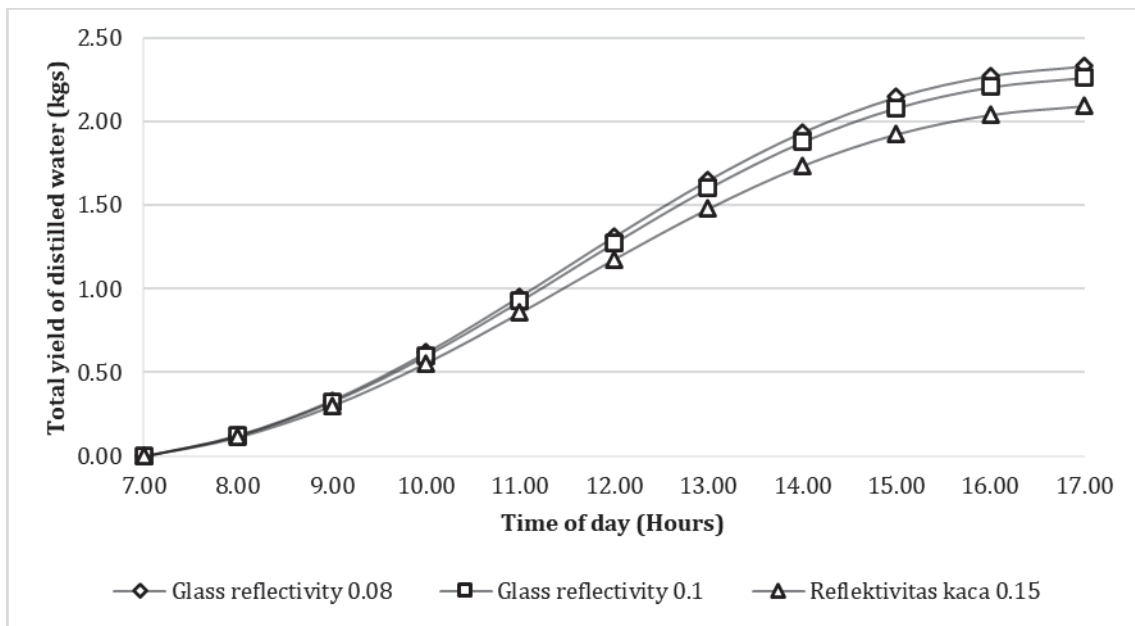


FIGURE 10. The total yield of distilled water from the glass reflectivity variation

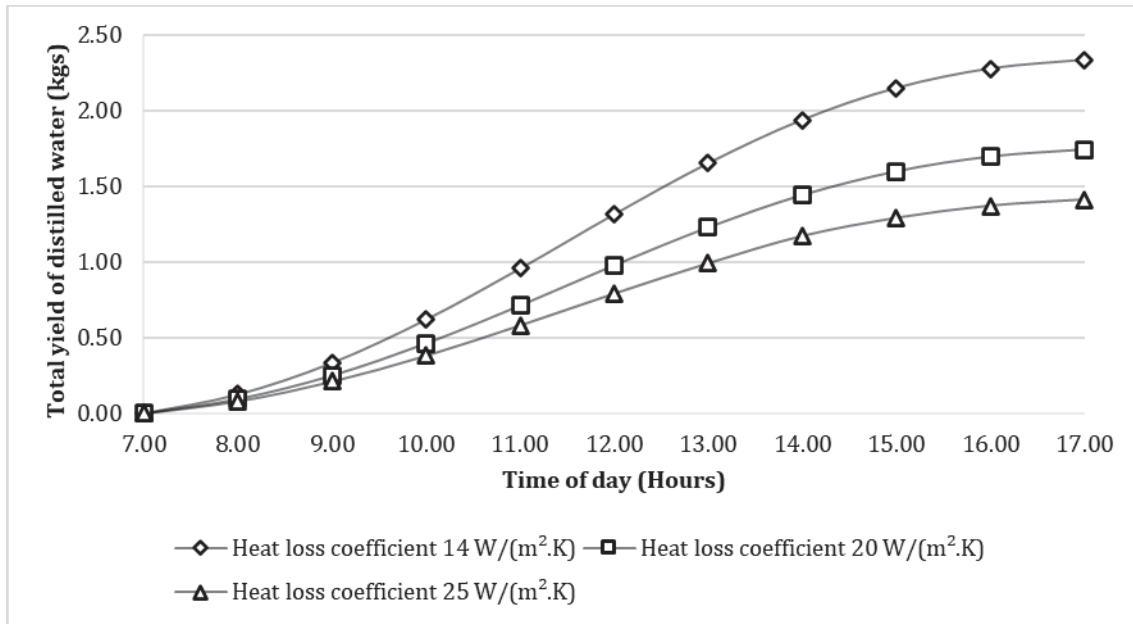


FIGURE 11. The total yield of distilled water from the heat loss coefficient variation

The highest total yield of distilled water was at the lowest water mass variation of 5 kg (Figure 7). It can be seen that the yield of distilled water decreases as the water mass inside the basin increases. The greater the water mass, the greater the energy needed to raise the water temperature. As a result, the water temperature becomes lower and harder to evaporate quickly. Thus, the solar still efficiency will be higher if the water mass inside the basin is less.

The highest total yield of distilled water was at the highest absorber absorptivity variation of 0.9 (Figure 8). It can be seen that the yield of distilled water increases as the absorber absorptivity increases. The absorber will more easily absorb heat so that the water temperature will quickly rise and the evaporation process is more effective due to the higher absorber absorptivity. The absorber absorptivity is determined by several factors such as the color and type of the absorber.

The highest total yield of distilled water was at the lowest glass absorptivity variation of 0.06 (Figure 9). It can be seen that the yield of distilled water decreases as the glass absorptivity increases. Due to the higher glass absorptivity, the glass temperature will quickly rise as a result of receiving more energy from solar radiation. The higher the glass temperature will affect the difficulty of the distilled water condensation process. Glass absorptivity is determined by several factors, such as the type of glass, the thickness of the glass and the clarity of the glass.

The highest total yield of distilled water was at the lowest glass reflectivity variation of 0.08 (Figure 10). It can be seen that the yield of distilled water increases as the glass reflectivity decreases. The higher the glass reflectivity, the lower solar radiation transmitted to the absorber so that the water temperature in the basin is difficult to rise and the water will take a longer time to evaporate. Like the glass absorptivity, the glass reflectivity is also determined by several factors, such as the type of glass, the thickness of the glass and the clarity of the glass.

The highest total yield of distilled water was at the lowest heat loss coefficient variation of 14 W/(m².K) (Figure 11). It can be seen that the yield of distilled water increases as the heat loss coefficient decreases. The loss referred to here is the heat energy loss that is discharged into the environment, so the lower the heat loss coefficient, the higher the thermal efficiency. Insulation material and geometry, the quality of the material and the solar still device along with the wind speed are factors that greatly influence the magnitude of the heat energy loss.

CONCLUSIONS

In this study, we analyzed and simulated the CSS performance with variations in some parameters such as water mass inside the basin, glass absorptivity, glass reflectivity, absorber absorptivity and heat loss coefficient. Mathematical models are used to calculate the yield of distilled water from the various variations mentioned to get the CSS model with the best results. The mathematical solution of the equations system is carried out by substitution and integration factors in the differential equation in each part of the device. Numerical solutions are carried out using the

Euler or Runge-Kutta method. There are several limitations to this study, the simulation only applies to conventional (unmodified) basin solar still model and under the steady-state process conditions. The results of this study obtained the following findings:

- The best results were achieved for the water mass inside the basin variations at the lowest water mass variation of 5 kg, with the total yield of distilled water of 2.33 kg.
- The best results were achieved for the absorber absorptivity variations at the highest absorber absorptivity variation of 0.9, with the total yield of distilled water of 2.33 kg.
- The best results were achieved for the glass absorptivity variations at the lowest glass absorptivity variation of 0.06, with the total yield of distilled water of 2.33 kg.
- The best results were achieved for the glass reflectivity variations at the lowest glass reflectivity variation of 0.08, with the total yield of distilled water of 2.33 kg.
- The best results were achieved for the heat loss coefficient variations at the lowest heat loss coefficient variation of 14 W/(m².K), with the total yield of distilled water of 2.33 kg.
- It can be concluded that TRNSYS is a very useful tool for the analysis and design of solar water distillation system.

This research could have future research directions such as the development of simulations for modified basin solar still models to increase efficiency and development of simulations for transient or unsteady state process conditions.

ACKNOWLEDGEMENTS

This study was conducted under the support of the Department of Mechanical Engineering, Sanata Dharma University.

REFERENCES

1. C. U. Maheswari and R. Meenakshi Reddy, "CFD Analysis of different types of single basin solar stills," *IOP Conf. Ser. Mater. Sci. Eng.*, vol. 330, no. 1, 2018, doi: 10.1088/1757-899X/330/1/012097.
2. J. T. Mahdi, B. E. Smith, and A. O. Sharif, "An experimental wick-type solar still system: Design and construction," *Desalination*, vol. 267, no. 2–3, pp. 233–238, 2011, doi: 10.1016/j.desal.2010.09.032.
3. M. S. Y. Ebaid and H. Ammari, "Modeling and analysis of unsteady-state thermal performance of a single-slope tilted solar still," *Renewables Wind. Water, Sol.*, vol. 2, no. 1, 2015, doi: 10.1186/s40807-015-0017-x.
4. J. A. Duffie and W. A. Beckman, *Solar Engineering of Thermal Processes*, Wiley, New York, 1991.
5. P. T. Tsilingiris, "Analysis of the heat and mass transfer processes in solar stills - The validation of a model," *Sol. Energy*, vol. 83, no. 3, pp. 420–431, 2009, doi: 10.1016/j.solener.2008.09.007.
6. A. E. Kabeel, S. A. El-Agouz, R. Sathyamurthy, and T. Arunkumar, "Augmenting the productivity of solar still using jute cloth knitted with sand heat energy storage," *Desalination*, vol. 443, no. May, pp. 122–129, 2018, doi: 10.1016/j.desal.2018.05.026.
7. P. Pal, P. Yadav, R. Dev, and D. Singh, "Performance analysis of modified basin type double slope multi-wick solar still," *Desalination*, vol. 422, no. June, pp. 68–82, 2017, doi: 10.1016/j.desal.2017.08.009.
8. P. Dumka, A. Sharma, Y. Kushwah, A. S. Raghav, and D. R. Mishra, "Performance evaluation of single slope solar still augmented with sand-filled cotton bags," *J. Energy Storage*, vol. 25, no. August, p. 100888, 2019, doi: 10.1016/j.est.2019.100888.
9. H. N. Panchal and P. K. Shah, "Modelling and verification of single slope solar still using ANSYS-CFX," *Int. J. Energy Environ.*, vol. 2, no. 6, pp. 985–998, 2011.
10. H. Ş. Aybar, "Mathematical modeling of an inclined solar water distillation system," *Desalination*, vol. 190, no. 1–3, pp. 63–70, 2006, doi: 10.1016/j.desal.2005.07.015.
11. Klein, S.A., et al., *TRNSYS, A Transient Simulation Program*, vol. 1, Solar Energy Laboratory, University of Wisconsin - Madison, USA, 2007.